Int. J. Electrochem. Sci., 15 **(2020)** 3347 – 3364, doi: 10.20964/2020.04.48

International Journal of ELECTROCHEMICAL SCIENCE
www.electrochemsci.org

Novel Potentiometric Sensors Based on ß-cyclodextrin and Dibenzo 18-crown-6 Ionophores/Mesoporous Silica Nanoparticles for Clidinium Determination

Sahar Mahmoud Mostafa[1,*], *Ahmed Ali Farghali* [2] *and Mohamed Magdy Khalil*[1]

[1] Chemistry Department, Faculty of Science, Beni-Suef University, Beni-Suef, Egypt.
[2] Materials Science and Nanotechnology Department, Faculty of Postgraduate Studies for Advanced Sciences, Beni-Suef University, Beni-Suef, Egypt.
[*]E-mail: dr_saharmahmoud888@yahoo.com

Received: 2 December 2019 / *Accepted:* 26 January 2020 / *Published:* 10 March 2020

For the first time, two novel potentiometric sensors based on ß-cyclodextrin/mesoporous silica nanoparticles (β-CD/MSNs-CPS, sensor I) and dibenzo 18-crown-6/mesoporous silica nanoparticles (DB18C6/MSNs-CPS, sensor II) were described for potentiometric determination of clidinium bromide (CDB). The sensor matrix optimization was focused on the nature and content of the sensing element, plasticizer, anionic additive and nanomaterials. The fabricated sensors showed linear, stable and Nernstian slopes of 59.9±0.5 and 56.6±0.3 mV decade^{-1} and detection limits of 6.8 x 10^{-8} and 9.0 x 10^{-8} mol L^{-1} for sensors I and II, respectively. The morphology and properties of sensors surface were characterized by scanning electron microscopy (SEM), transmission electron microscopy (TEM) and electrochemical impedance spectroscopy (EIS), respectively. The sensors were found to be accurate and usable within wide pH range (4.0-11.5) in short response times (4 and 8 s). The thermal stability coefficients of the investigated sensors were 0.00041 and 0.00032 V ^{o}C^{-1}. The sensors showed adequate selectivity against some inorganic cations and were felicitously implemented for CDB determination in pure solutions, pharmaceutical preparation, biological fluids and surface water samples.

Keywords: Carbon paste sensors; Clidinium bromide; Mesoporous silica nanoparticles; Pharmaceutical analysis; Surface water

1. INTRODUCTION

Drug analysis and development of better methods for achieving this target are of critical importance for drug quality control as well as clinical treatment [1].

Clidinium bromide (CDB), 3-[(2-hydroxy-2,2-diphenylacetyl)oxy]-1-methyl-1-azabicyclo [2.2.2] octan-1-ium bromide (Figure 1) is an anticholinergic drug that inhibits the activity of

acetylcholine neurotransmitter in central and peripheral nervous system synapses. This prevents symptoms of cramping and abdominal / stomach pain by reducing stomach acid and slowing down the intestines. Different methods were applied for clidinium determination including high performance liquid chromatography [2-3], derivative spectroscopy [4,5], spectrophotometric methods [6,7], capillary electrophoresis [8] and kinetic spectrophotometric methods [9], The majority of these methods include one or more defects such as narrow concentration range [2,8], low sensitivity and robustness for biological samples [8], time consuming [8] and low precision [7]. Therefore, our goal aimed to avoid wasting time, cost and sensitivity for CDB micro determination using potentiometric sensors [10-13]. Careful investigation of the literature showed that only a poly vinylchloride (PVC) sensor based on ion-pair associates of CDB with tetraphenyl borate was published [14].

Mesaric and Damen [15] were the first to use carbon paste-filled sensors. Compared with polymeric membrane sensors, carbon paste sensors (CPSs) attracted a great deal of attention due to their high sensitivity, low ohmic resistance, renewability, stable response, chemical inertness, ease of chemical or biological modification and no need for internal filling solution [16,17].

Based on the formation of inclusion complexes between cyclodextrins and drug cations [18-20], potentiometric sensors utilizing β-CD as sensing ionophore for CDB micro determination can be tested. Also, the use of crown ethers ionophores in the fabrication of a liquid membrane [21], solid state [22] and screen printed [23] potentiometric sensors for drug cations determination is very limited.

Recently, nanomaterials attracted considerable attention as suitable materials for modification the surface of potentiometric sensors because of their interesting physicochemical properties, which differ significantly from those shown by the same bulk materials [24-28]. For example, mesoporous silica nanoparticles (MSNs) have unique properties such as high surface area, customizable pore diameter (2-50 nm), straightforward synthesis, easy functioning of their surfaces by functional groups, high chemical and biological stability, and good biocompatibility [29-34].

Due to the above mentioned properties, we decided to use mesoporous silica nanoparticles (MSNs), in our current research aiming to improve the detection limit and stability of the investigated sensors. The study is based on fabrication of two novel sensors, the first sensor includes β-CD as ionophore incorporating MSNs whereas the second sensor includes dibenzo-18-crown-6 as ionophore incorporated with the same nanoparticle. The constructed sensors were used successfully for CDB determination in pharmaceutical compounds, biological fluids and surface water samples.

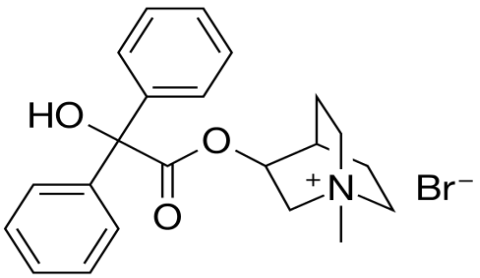

Figure 1. Chemical structure of clidinium bromide.

2. EXPERIMENTAL

2.1. Reagents and materials

In this work, all high purity chemicals and reagents were used. Deionized water (DW) was used to prepare all the solutions. Different cyclic macro molecules were tested as sensing ionophores including β-cyclodextrin (β-CD), dibenzo-18-crown-6 (DB18C6), 18-crown-6 (18C6) (Euromedex, France) and chitosan (CH, biobasic, Canada INC, with a degree of de-acetylation 96%).

The sensor plasticizers were as following**:** dioctyl adipate (DOA, Fluka, U.S.A), dibutyl phthalate (DBP), dioctyl phthalate (DOP), acetophenone (AP) and dimethyl phthalate (DMP) (Merck, Germany). Sodium tetraphenylborate (NaTPB, Fluka, U.S.A) was used as anionic site. The metal salts were provided by BDH as nitrates or chlorides. Spectroscopic graphite powder (1-2 mm, Sigma Aldrich) was applied as sensors materials.

2.2. Authentic samples

Pure-grade clidinium bromide (CDB) ($C_{22}H_{26}BrNO_3$, M.Wt = 432.358 g mol^{-1}) has been supplied by the Egyptian International Pharmaceutical Industries Company (EIPICO, 10^{th} of Ramadan City, Egypt). The preparation of stock solution (1.0×10^{-2} mol L^{-1}) was carried out by dissolving an appropriate amount of CDB in deionized water. Working solutions covering the concentration range from 1.0×10^{-2} to 1.0×10^{-8} mol L^{-1} were prepared by appropriate dilution.

2.3. Pharmaceutical preparations

The pharmaceutical product (Librax) was purchased from local drug stores.

2.4. Biological samples

Aliquots of biological fluid (urine or plasma, obtained from a healthy male) have been spiked with different concentrations of CDB.

2.5. Surface water samples

Aliquots of surface water obtained from an area in the River Nile (Beni-Suef City, Egypt) were transferred to a 100 mL beaker and spiked with different CDB concentrations.

2.6. Apparatus

Potentiometric and pH-measurements were carried out using a 702 SM titrino (Metrohm, Switzerland). The temperature of the investigated solutions was controlled by using a mLw W20 circulator thermostat. The electrochemical impedance spectroscopy (EIS) was measured in an

analytical system, with Autolab PGSTAT 302 N (Metrohm). SEM (Quanta FEG-250 SEM, Switzerland) and TEM (JEOL-JEM 2100, Japan) images were used for characterization of sensors morphology.

2.7. Synthesis of mesoporous silica nanoparticles (MSNs)

MSNs were prepared applying Moon et al method [35] with some modifications. In a typical synthesis, 1 g of cetylpyridinium bromide (CPB) and 0.6 g of urea were dissolved in 30 mL of deionized water and stirred for 30 min. Subsequently, 30 mL of cyclohexane and 1.2 mL of isopropanol were added to the solution. 2.7 mL of tetraethyl orthosilicate (TEOS) to the mixed solution was added dropewise to the mixed solution over 5 min. with vigorous stirring. After 30 min. of vigorous stirring, the mixture was heated to 85 ° C and then kept for 17 hrs. For MSNs collection, the mixture was centrifuged and washed several times with acetone and water. Finally, MSNs were left to dry at room temperature for 12 hrs and calcined at 600 ° C for 6 hrs in the air to remove the surfactant template. Characterization of the resulting material was performed using SEM and TEM (Figure 2).

2.8. Sensors fabrication

The CP sensors were fabricated as mentioned previously [36]. The influence of lipophilic anionic additive and mesoporous silica nanoparticles on the performance characteristics of the examined sensors was studied by adding variable percentages of NaTPB and MSNs. The sensors were preconditioned for 1 hr in a 1.0×10^{-3} mol L^{-1} clidinium bromide solution.

2.9. Analytical applications

Potentiometric titration was carried out by transferring different volumes (1–5 mL) of $1,0\times10^{-2}$ mol L^{-1} drug solution to a 50 mL beaker and then titrated with NaTPB. Applying the standard addition method, small increments of 1.0×10^{-2} mol L^{-1} of CDB solution were added to 50 mLaliquot samples of different concentrations of pure drug and pharmaceutical formulation. Various concentrations of CDB containing 5 mL of plasma or urine from a healthy person and surface water samples from the River Nile (Beni-Suef City, Egypt) were prepared and subjected to standard addition method.

3. RESULTS AND DISCUSSION

3.1. Characterization of MSNs

Figure 2(a) showed SEM image of non-aggregated spherical particles with almost uniform sizes (~50 nm). For confirmation, TEM image (Figure 2(b)) demonstrated spherical shape and well dispersion of MSNs nanoparticles with dendrimeric fibers coming out from the center and scattered uniformly in all directions.

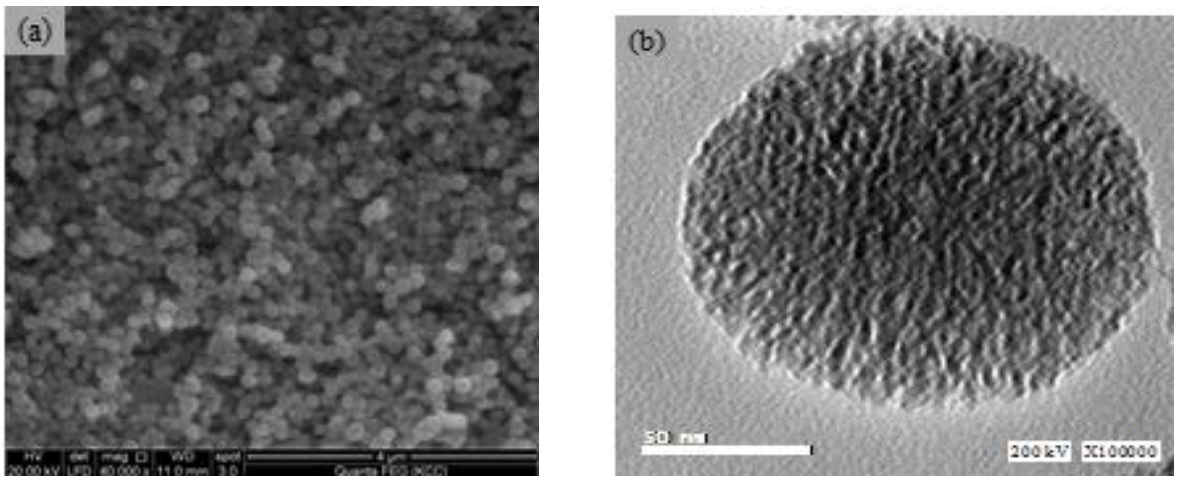

Figure 2. Characterization of MSNs. (a) SEM and (b) TEM.

3.2. Optimal sensor matrices compositions

Comprehensive studies were carried out on the sensing matrix composition concerning the nature and amount of sensing ionophore, lipophilic anionic additive, plasticizer and MSNs aiming to achieve the highest potentiometric performance (Table 2).

3.2.1. Effect of sensing ionophores

The sensitivity and selectivity of potentiometric sensors based on ionophores is usually governed by the complexation between the target analyte and the molecular recognition element. In the present study, different ionophores (β-CD, dibenzo 18-crown-6, 18-crown-6 and chitosan) were tested. The obtained results revealed that sensors based on β-CD or dibenzo 18-crown-6 ionophores exhibited best potentiometric response compared with those based on the other ionophores. This may be attributed to stable inclusion complex formation between ionophores and the target drug cation as mentioned previously in the introduction.

3.2.2. Effect of ionophore percentage

In fact, the percentage of ionophore in carbon paste composition affects significantly the sensitivity and linearity for a given cation. The data (Table 1) showed that sensors incroporating 0.5 wt % ionophore (β-CD or dibenzo 18-crown-6) exhibited the highest sensitivity toward CD^+ cation. However, further addition of ionophore led to lowering in potentiometric response to some extent. This behaviour may be attributed to some inhomogenities and paste saturation; the paste resistance increased.

3.2.3. Effect of anionic additives

Stabilization of charged complexes and ensuring the permselectivity and electroneutrality of the paste were achieved by the incorporation of MSNs. Also, the interfacial ion-exchange kinetics at the sensor surface as well as the ionic mobility in the sensor matrix were enhanced by incorporating NaTPB in the paste containing 0.5 wt% β-CD. Addition of 0.3 wt% NaTPB caused an increase of slope 49.9 ± 0.5 to 55.7 ± 0.4 mV/decade and a decrease of detection limit from 1.9 x 10^{-6} to 1.5 x 10^{-6} mol L^{-1}. No reasonable effect on the sensor response was observed by further addition of NaTPB as shown in Table 1.

Different graphite/DBP ratios with fixed amounts of ionophore and anionic additive were examined. The best sensitivity and reproducibilty of the investigated sensors were achieved by using 49.45/49.75 (g/p) ratio owing to the optimum physical properties and adequate mobilities of paste components.

3.2.4. MSNs impact on sensor performance

The electrochemical behaviour of the examined sensors was enhanced by incorporating MSNs in the composition of the paste. Addition of different percentages of MSNs (0.3 to 10 % (w/w relative to carbon powder) in the paste matrix containing 0.5% ionophore and 0.3%NaTPB was examined. It is obvious that the Nernstian slope was improved (59.9±0.5 and 56.6±0.3 mV $decade^{-1}$) and the detection limits decreased (6.8x10^{-8} and 9.0x10^{-8} mol L^{-1}) for sensors I and II, respectively (Figure 3). However, further increase the amount of MSNs displayed declining behaviour.

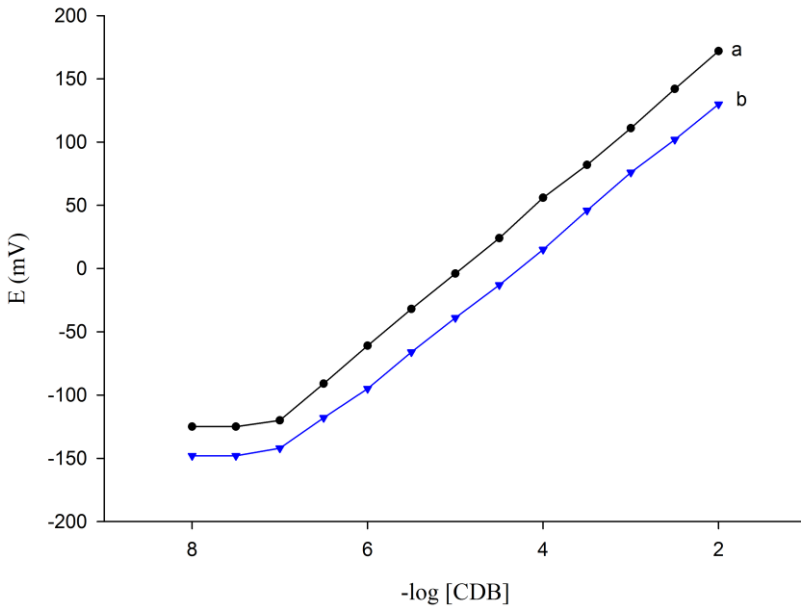

Figure 3. Calibration curves of (a) β-CD/MSNs-CPS (sensor I) and (b) DB18C6/MSNs-CPS (sensor II) at optimum paste composition.

Table 1. Optimization of sensors composition and their potentiometric response.

	Composition (%)				Sensor characteristics				
Sensor No.	G	Ionophore	A	MSNs	Slope (mV/decade)	LR (mol L^{-1})	DL (mol L^{-1})	r^2	RSD (%)
1	50.00	-	-	-	33.5±0.5	$9.5 \times 10^{-6} – 1.0 \times 10^{-2}$	7.9×10^{-6}	0.999	0.87
2	49.85	0.3 β-CD	-	-	42.8±0.8	$3.9 \times 10^{-5} – 1.0 \times 10^{-2}$	3.2×10^{-6}	0.964	1.09
3	59.80	0.4 β-CD	-	-	45.1±0.2	$3.1 \times 10^{-5} – 1.0 \times 10^{-2}$	2.5×10^{-6}	0.997	0.27
4	**49.75**	**0.5** β-CD	-	-	**49.9±0.5**	**$8.4 \times 10^{-6} – 1.0 \times 10^{-2}$**	**1.9×10^{-6}**	**0.999**	**0.56**
5	49.70	0.6 β-CD	-	-	46.9±0.9	$8.8 \times 10^{-6} – 1.0 \times 10^{-2}$	3.9×10^{-6}	0.995	1.12
6	49.65	0.7 β-CD	-	-	46.0±0.5	$1.1 \times 10^{-5} – 1.0 \times 10^{-2}$	4.8×10^{-6}	0.994	0.98
7	49.50	1.0 β-CD	-	-	44.2±0.2	$5.6 \times 10^{-5} – 1.0 \times 10^{-2}$	8.5×10^{-6}	0.995	0.26
8	49.65	0.5 β-CD	0.1 NaTPB	-	53.4±0.3	$1.1 \times 10^{-5} – 1.0 \times 10^{-2}$	1.7×10^{-6}	0.979	0.65
9	**49.45**	**0.5 β-CD**	**0.3 NaTPB**	**-**	**55.7±0.4**	**$9.5 \times 10^{-6} – 1.0 \times 10^{-2}$**	**1.5×10^{-6}**	**0.999**	**0.42**
10	49.25	0.5 β-CD	0.5 NaTPB	-	70.2±0.2	$8.8 \times 10^{-6} – 1.0 \times 10^{-2}$	1.8×10^{-6}	0.987	0.17
11	49.05	0.5 β-CD	0.7 NaTPB	-	70.6±0.3	$9.9 \times 10^{-6} – 1.0 \times 10^{-2}$	2.5×10^{-6}	0.991	0.25
12	49.15	0.5 β-CD	0.3 NaTPB	0.3	52.7±0.2	$7.8 \times 10^{-6} – 1.0 \times 10^{-2}$	3.1×10^{-6}	0.990	0.22
13*	**48.95**	**0.5 β-CD**	**0.3 NaTPB**	**0.5**	**59.9±0.5**	**$9.9 \times 10^{-8} – 1.0 \times 10^{-2}$**	**6.8×10^{-8}**	**0.999**	**0.40**
14	44.45	0.5 β-CD	0.3 NaTPB	5.0	56.9±0.4	$2.3 \times 10^{-6} – 1.0 \times 10^{-2}$	7.7×10^{-7}	0.997	0.41
15	39.45	0.5 β-CD	0.3 NaTPB	10.0	48.8±0.1	$2.5 \times 10^{-5} – 1.0 \times 10^{-2}$	6.6×10^{-6}	0.990	0.12
16*	**48.95**	**0.5 DB18C6**	**0.3 NaTPB**	**0.5**	**56.6±0.3**	**$2.9 \times 10^{-7} – 1.0 \times 10^{-2}$**	**9.0×10^{-8}**	**0.999**	**0.61**
17	48.95	0.5 18C6	0.3 NaTPB	0.5	55.5±0.3	$9.6 \times 10^{-6} – 1.0 \times 10^{-2}$	5.1×10^{-7}	0.999	0.52
18	43.95	0.5 CH	0.3 NaTPB	0.5	47.2±0.2	$8.9 \times 10^{-6} – 1.0 \times 10^{-2}$	5.1×10^{-7}	0.999	0.25

G: Graphite, A: Anionic additive, LR: Linear range, DL: Detection limit, r2: Correlation coefficient, RSD: Relative standard deviation

Table 2. Optimization and electrochemical response characteristics of the proposed CDB sensors.

Parameter	Sensor I	Sensor II
Slope (mV $decade^{-1}$)	59.9±0.5	56.6±0.3
Composition (%)	0.5% β-CD +0.3% NaTPB +0.5% MSNs +48.95% G +49.75%DBP	0.5 % DB18C6 + 0.3% NaTPB + 0.5% MSNs + 48.95% G +49.75%DBP
Graphite/ Plasticizer ratio	0.99	0.99
Concentration range (mol L^{-1})	$9.9 \times 10^{-8} – 1.0 \times 10^{-2}$	$2.9 \times 10^{-7} – 1.0 \times 10^{-2}$
Detection limit (mol L^{-1})	6.8×10^{-8}	9.0×10^{-8}
Quantification limit (mol L^{-1})	2.3×10^{-7}	3.0×10^{-7}
Correlation coefficient (r^2)	0.999	0.999
RSD (%)	0.40	0.61
Response time (s)	4	8
Thermal coefficient ($V/^0C$)	0.00041	0.00032
Working pH range	4.0 -11.5	4.0 -11.5
Life time (days)	70	60

3.3. Characterization of sensors surface

The sensor surface morphology plays a vital role in selectivity as well as sensitivity of the assayed ion. Figure 4 showed SEM images of the morphological features of the investigated sensors. The unmodified CPS is characterized by a surface formed by irregularly shaped graphite falkes, which were isolated and a closer look of the film reveales a broken surface (Figure 4a). After modification of

the CPS with MSNs nanoparticles, it can be seen that non-aggregated spherical particles of MSNs were distributed on the sensor surface (Figure 4b). In addition, HRTEM was applied for the proposed sensors to confirm the high distribution of MSNs on graphite layers (Figure 4c, d).

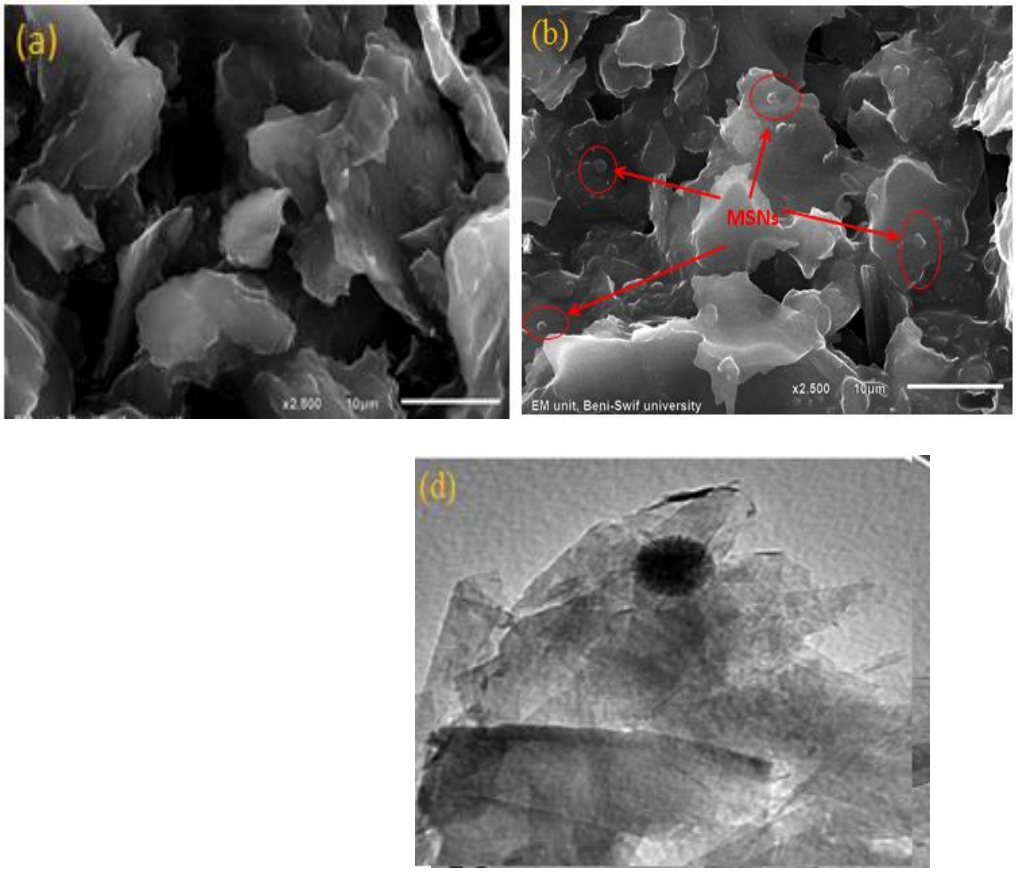

Figure 4. SEM image of β-CD-CPS (a), SEM image of β-CD/MSNs-CPS (b), TEM image of β-CD/MSNs-CPS (c) and TEM image of DB18C6/MSNs-CPS (d).

3.4. Characterization by electrochemical impedance spectroscopy (EIS)

Applying EIS measurements facilitated the description of sensor processes and exploration of MSNs effect on the conductivity property of the sensor surface and the study of electrochemical kinetics at the sensor/electrolyte interface. The proposed sensors in $[Fe(CN)_6]^{-3/-4}$ solution containing 0.1 mol L^{-1} KNO_3 were investigated using EIS measurements as shown in Figure 5A. The measurements were carried out at an open-circuit with amplitude of 1.5 mV and a frequency range from (10000 - 0.1) Hz. Figure 5B demonstrated the recognition of electrical properties of the sensor / solution interface by using an equivalent circuit. The value of each electrical element in the equivalent circuit was obtained by fitting the electrochemical impedence spectra to the equivalent circuit. Incorporation of 0.5% MSNs caused lowering of the semicircle diameter from 2.27 to 0.706 and 0.971 to 0.402 kΩ for sensors I and II, respectively. The potential response of the sensors was improved by increasing the paste surface conductivity.

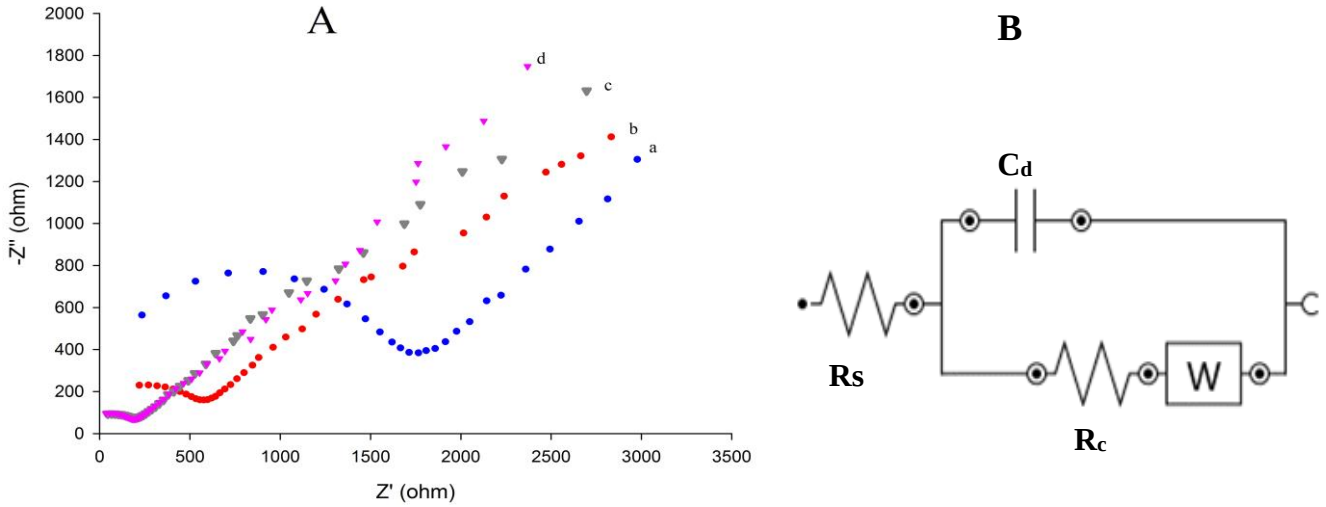

Figure 5. (A) Impedance plots for different sensors in $[Fe(CN)_6]^{-3/-4}$ containing 0.1 mol L^{-1} KNO_3: (a) unmodified β-CD-CPS, (b) unmodified DB18C6-CPS, (c) β-CD/MSNs-CPS and (d) DB18C6/MSNs-CPS and (B) Equivalent circuit.

3.5. Effect of plasticizer

The plasticizer plays an important role for dissolving the ionophores and NaTPB present in the paste. The dielectric constant of the paste and the relatively high mobility of the paste constituents were affected by the plasticizers. Various equilibria between ionophores and drug cation in the paste phase were also controlled by the plasticizer type. Lipophilicity, volatility, viscosity , molecular weight and cost are other important factors which can be considered besides the dielectric constant. Different plasticizers (DBP, DOP, DOA, AP, DMP, Almond, Coconut, Olive and Sunflower) covering a very wide dielectric constants range (ε_r 3.1 - 17.4) were investigated. The best potential response was achieved for the sensor plasticized with the DBP (ε_r 6.4) compared with the other plasticizers tested [37]. It is worth mentioning that the sensor plasticized with AP (ε_r 17.4) exhibited a poor potentiometric response which can be ascribed to its high volatility and water solubility.

3.6. Response time, reversibility and repeatability of sensors

The dynamic response times were found to be 4 and 8 s over a concentration range 1.0×10^{-7}-1.0×10^{-2} mol L^{-1} for sensors I and II, respectively (Figure 6). It is obvious to note that the presence of MSNs improved the sensor conductivity and increased the transduction properties which led to the fast response time of the sensors.

Careful evaluation of the sensors reversibility was performed by a similar procedure in the opposite direction (1.0×10^{-2}-1.0×10^{-7} mol L^{-1}) drug concentrations indicating the reversibility of the sensors response.

Investigation of repeatability of the potential reading for the investigated sensors was carried out in 1.0×10^{-4} mol L^{-1} CDB solution shortly after measuring the first set of solutions at 1.0×10^{-3} mol L^{-1}. The high precision of the sensors with no memory effect can be attributed to the low R. S. D. values (0.52 and 0.78) of five reproducing measurements.

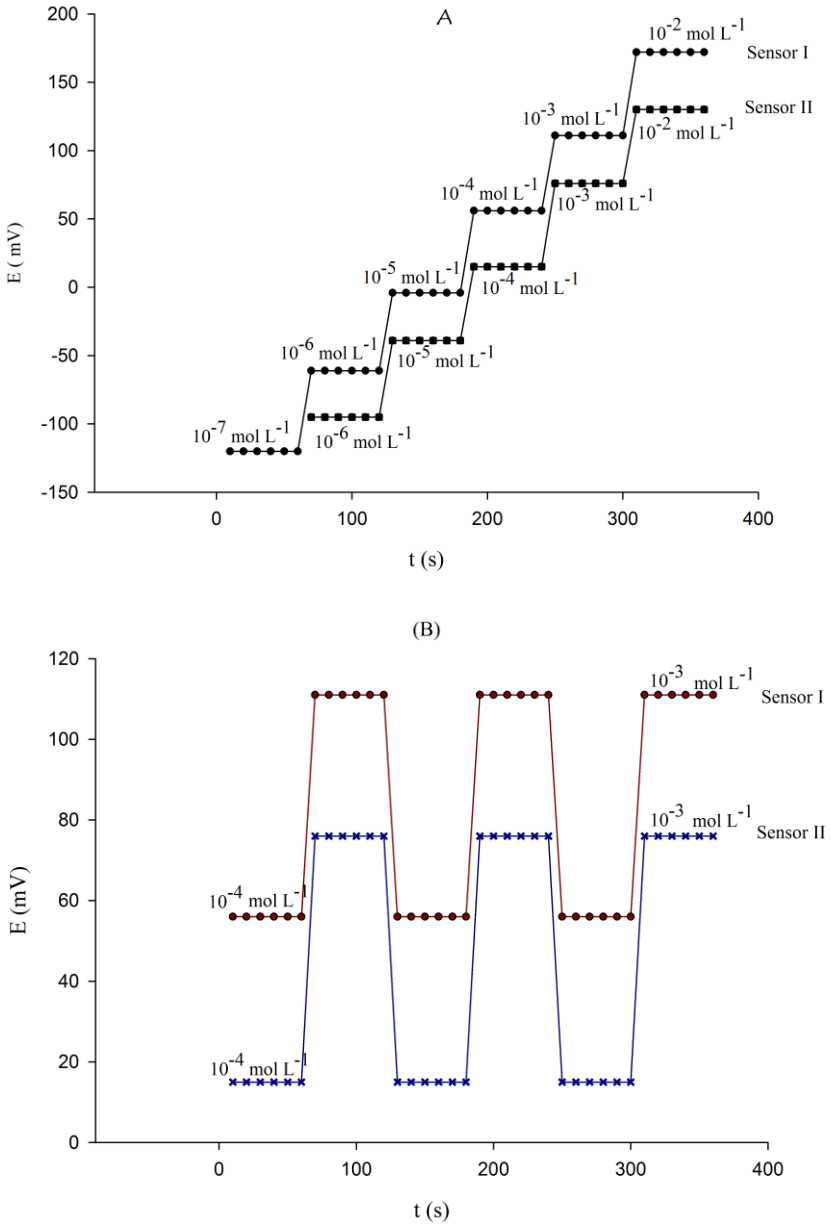

Figure 6. Dynamic response time of different CDB sensors (A) for step change in concentrations of CDB from low to high and (B) for several low-to-high sample cycles for sensors I and II.

3.7. Lifetime and regeneration of the sensors

Lifetimes of the investigated sensors (I and II) were found to be 70 and 60 days, respectively during which the sensors displayed a slight gradual decrease in slope and an increarse in the detection limit.

The regeneration of the CDB sensors was achieved as described previously [38]. The calibration curves for exhausted sensors showed (slopes 37.2 and 38.4 mV decade^{-1}) and after regeneration (slopes 52.6 and 51.0 mV decade^{-1}) for sensors I and II, respectively (Figure 7). The data revealed that the life span of the regenerated sensors is limited to 6 hrs. This can be ascribed to the ease of leaching of the sensing material at the sensor surface.

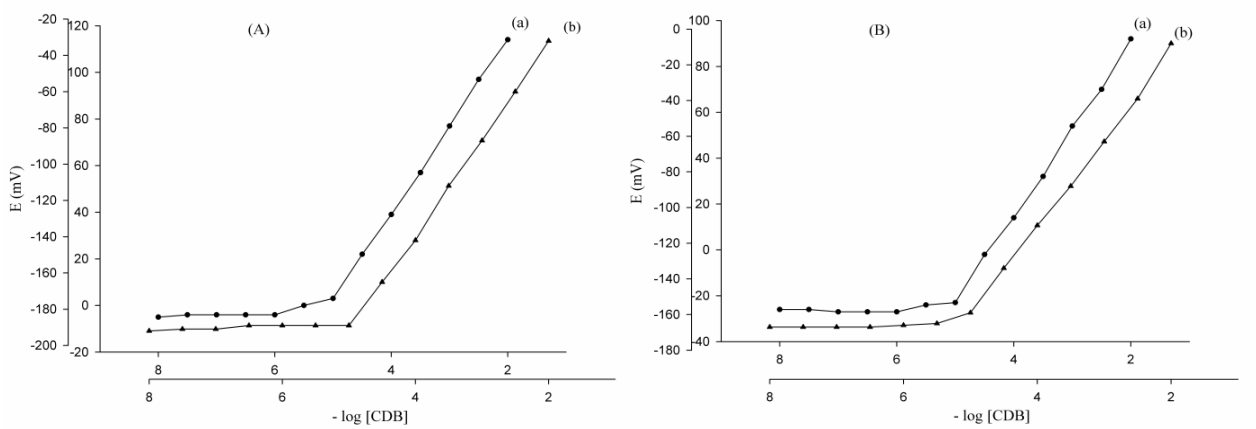

Figure 7. Calibration curves of sensor I (A) and sensor II (B): (a) expired and (b) regenerated sensors.

3.8 Effect of pH

SPECIES program [39] was used for plotting the percent species of drug as a function of pH to investigate the ionized and non-ionized species in solution (Figure 8). Since pKa of clidinium is 11.05 , therefore at pH 10.4 the drug will be in the cationic form.

The pH dependence of the sensors for 1.0×10^{-5}, 1.0×10^{-4} and 1.0×10^{-3} mol L^{-1} CDB concentrations was tested in a pH range 2.0-12.0. The potential response remained constant over the pH range of 4.0–11.5 (Figure 9a, b).

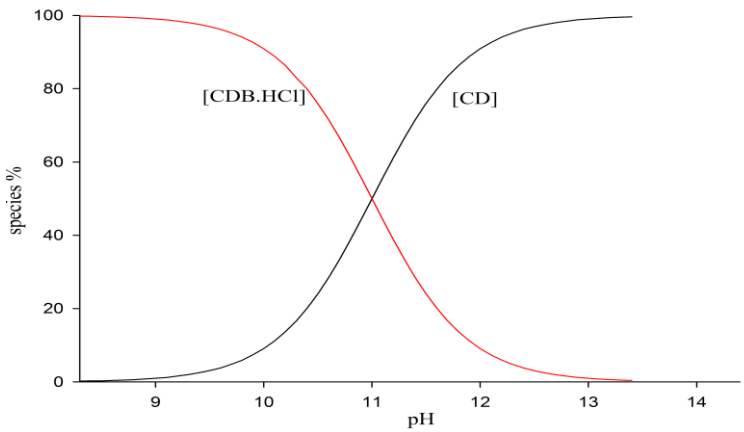

Figure 8. Representative concentration distribution diagram for CDB species.

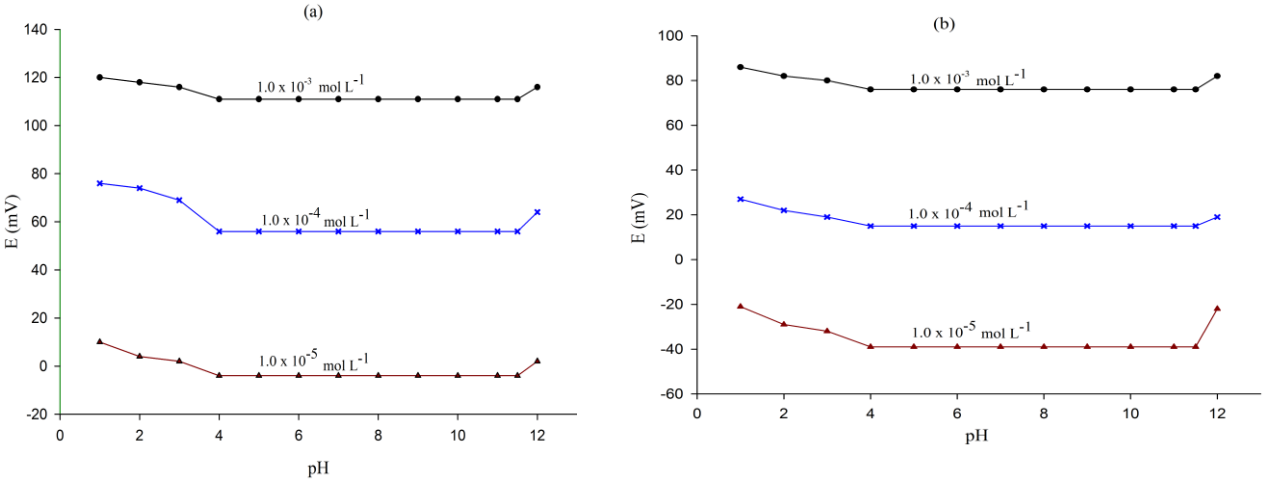

Figure 9. Effect of pH on the potential response of investigated sensors.

3.9. Effect of temperature

The calibration curves of the sensors were constructed at different temperatures (20–60 ^{o}C). The data revealed that the sensors have very small thermal temperature coefficients values (0.00041 and 0.00032 V/^{o}C) indicating the high thermal stability of the sensors within the investigated temperature range.

3.10. Selectivity

The selectivity parameter of the examined sensors was tested towards some selected inorganic cations, sugars and amino acids using the separate solution and the matched potential methods [40-42]. The data shown in Table 3 revealed that the selectivity coefficient values for sensor I were found to be slightly lower than those for sensor II, indicating the relatively high selectivity of the former sensor.

Confirmation of the selectivity behaviour of the sensors towards inorganic cations was performed applying an excellent approach called Bakker protocol [43-45]. The calibration curves were prepared by plotting the potential response of sensors against -log [species] (Figure 10). The data revealed that there was no noticeable response for all interfering species tested confirming the high selectivity of the examined sensors.

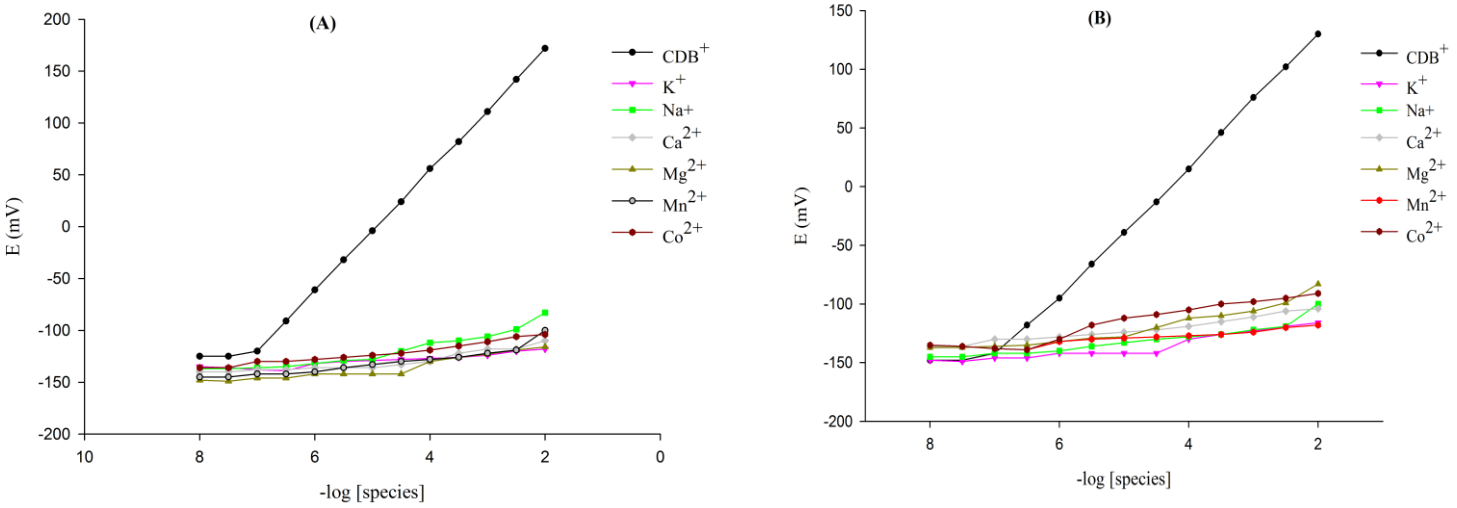

Figure 10. Response to CDB and certain interfering species using (A) sensor I and (B) sensor II.

Table 3. Selectivity coefficient $K_{CDB,\,j}^{\,pot}$ of of the proposed sensors.

	$K_{CDB,\,j}^{\,pot}$			
	Sensor I		Sensor II	
Interferent	SSM	MPM	SSM	MPM
K^+	1.9×10^{-3}	---	8.1×10^{-2}	---
Na^+	9.2×10^{-4}	---	6.9×10^{-1}	---
Ca^{2+}	4.1×10^{-5}	---	5.2×10^{-3}	---
Mg^{2+}	5.0×10^{-5}	---	6.4×10^{-3}	---
Co^{2+}	1.2×10^{-4}	---	1.3×10^{-2}	---
Mn^{2+}	3.5×10^{-5}	---	1.2×10^{-2}	---
Glucose	---	3.9×10^{-3}	---	2.2×10^{-2}
Maltose	---	4.8×10^{-3}	---	1.2×10^{-2}
Glycine	---	4.8×10^{-3}	---	1.1×10^{-2}
β-alanine	---	5.3×10^{-3}	---	1.2×10^{-2}

3.11. Stability of the sensors

In-depth examination concerning the stability of sensors I and II was performed by measuring the potentiometric response daily applying 5.0 x 10^{-6} mol L^{-1}. Fortunately, the proposed sensors retained 97% of its initial concentration for more than 7 and 5 weeks. The data revealed that the modified sensors acquired excellent stability (R. S. D values 0.4 and 0.61%) compared with other sensors published recently [14,18, 46] .

3.12. Analytical applications

The investigated sensors were used successfully in analytical applications for CDB determination in pure solutions, commercially available pharmaceutical formulations, biological fluids and surface water samples applying potentiometric titration and standard addition methods. Figure 11 displayed potentiometric titration and differential curves for sensor I as a representative; indicating accurate determination of CD^{+} ion. The obtained recovery values ranged from 96.60 to 101.40% and 96.00 to 101.78%, with R. S. D values of 0.12-1.76 and 0.04-2.20% using sensors I and II, respectively (Table 4). As seen in Table 5, the values of F-and t-tests were less than the tabulated ones confirming the high precision and accuracy of the proposed sensors.

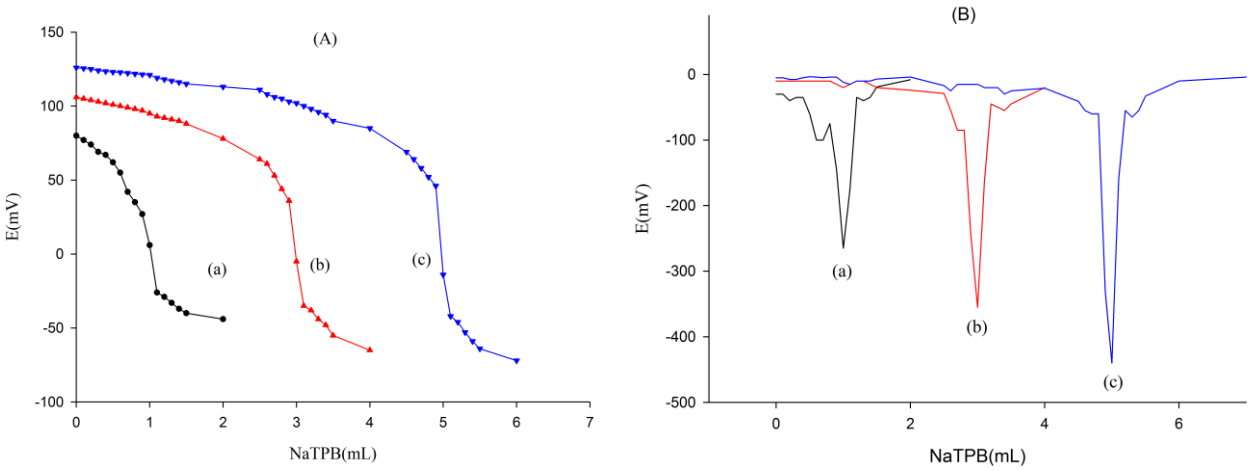

Figure 11. (A) Potentiometric titration curves of (a) 1, (b) 3 and (c) 5 mL of 10^{-2}mol L^{-1} CDB using sensor I and 10^{-2}mol L^{-1} NaTPB as titrant and (B) its first order derivative.

Table 4. Determination of CDB applying the standard addition method.

Sample	Standard addition method		
	Taken (mg)	Recovery (%)	RSD (%)
	Sensor I		
Pure solution	0.22	100.0	0.12
	2.16	99.66	1.65
	4.32	99.97	0.26
Mean±SD		99.9±0.19	
Librax	0.22	99.83	0.85
	2.16	99.13	1.33
	4.32	99.11	1.38
Mean±SD		99.4±0.41	
Spiked plasma	0.22	100.20	0.36
	2.16	101.40	2.39
	4.32	96.60	0.56
Mean±SD		99.4±2.50	
Spiked urine	0.22	100.00	0.49
	2.16	99.20	0.29
	4.32	100.00	0.06
Mean±SD		99.7±0.46	
Surface water	0.22	98.70	0.91

	2,16	97.00	0.42
	4.32	99.30	1.76
Mean±SD		98.3±1.21	
	Sensor II		
Pure solution	0.22	99.55	0.77
	2.16	98.88	0.56
	4.32	97.81	0.70
Mean±SD		98.7±0.89	
Librax	0.22	99.27	0.91
	2.16	99.80	1.31
	4.32	99.60	0.76
Mean±SD		99.6±0.27	
Spiked plasma	0.22	97.30	0.56
	2.16	98.40	2.05
	4.32	96.00	0.04
Mean±SD		97.2±1.24	
Spiked urine	0.22	98.88	2.20
	2.16	101.78	0.51
	4.32	99.27	0.99
Mean±SD		100.0±1.60	
Surface water	0.22	100.00	1.13
	2.16	99.30	0.52
	4.32	98.20	0.30
Mean±SD		99.2±0.92	

Table 5. Statistical comparison between the results of an analysis of CDB applying the standard addition and potentiometric titration methods.

Parameters	Standard addition method	Potentiometric titration method
	Sensor I	
Mean recovery (%)	99.90 [a]	99.70 [b]
SD [c]	0.19	0.27
RSD (%)	0.19	0.28
F-ratio	2.02 (9.20) [d]	
t-test	1.25 (2.77) [e]	
	Sensor II	
Mean recovery (%)	98.70 [a]	99.80 [b]
SD [c]	0.89	0.52
RSD (%)	0.89	0.53
F-ratio	2.93 (9.20) [d]	
t-test	1.29 (2.77) [e]	

[a] ; Average of four determinations, [b]; Average of three determinatios, [c]; Standard deviation, [d]; Tabulated F-value at 95% confidence level, [e] ; Tabulated t-value at 95% confidence level and four degrees of freedom.

3. 13. Comparison study

Recently, carbon paste sensors were used to overcome the inherent limitations of polymeric membrane sensors based on ion-pairs [14]. The limited selectivity of the latter sensors restricted their

application in complex biological samples. Improvement of both sensitivity and selectivity was achieved by the formation of inclusion complex between the ionophore and the target analyte. The fabricated sensors showed lower DL, 6.8×10^{-8} and 9.0×10^{-8}, wide pH range 4-11.5, fast response time (4 and 8 s), long lifetimes and high thermal stability (0.00041 and 0.00032 V/^{o}C) with excellent recovery (100 %) and RSD (0.06 %) compared with published methods [2, 6] and PVC membrane sensor [14] as shown in Table 6.

Table 6. Comparison between the proposed clidinium sensors and some of the other published methods.

Method	LR mol L^{-1}	DL mol L^{-1}	Slope mV $decade^{-1}$	pH	Response time (s)	r^2	RSD %	Ref
RP-HPLC	3.5×10^{-5}–5.8×10^{-5}	1.9×10^{-6}	25.09	----	----	0.998	1.40	[2]
Spectrophotometric methods	1.2×10^{-6}–3.5×10^{-5}	8.6×10^{-7}	---	----	----	0.9997	0.44	[6]
Potentiometric sensors								
PVC membrane	1.0×10^{-5} –1.0×10^{-1}	1.0×10^{-5}	57.0±0.3	4.0-10.0	20	0.9999	4.50	[14]
Sensor I	9.9×10^{-8} –1.0×10^{-2}	6.8×10^{-8}	59.9±0.5	4.0-11.5	4	0.9999	0.40	[P.W]
Sensor II	2.9×10^{-7} –1.0×10^{-2}	9.0×10^{-8}	56.6±0.3	4.0-11.5	8	0.9999	0.61	[P.W]

P.W: Present work.

4. CONCLUSION

The present study describes the fabrication of two novel sensors based on ß-CD or DB18C6 as sensing ionophores for potentiometric determination of clidinium bromide. The prepared sensors exhibited Nernstian slope of 59.9±0.5 and 56.6±0.3mV $decade^{-1}$ over a wide rang of concentrations range of 9.9×10^{-8} – 1.0×10^{-2} and 2.9×10^{-7} – 1.0×10^{-2} mol L^{-1} with lower detection limits of 6.8×10^{-8} and 9.0×10^{-8} mol L^{-1} in fast response time and wide pH range 4.0–11.5. The unique properties of the MSN nanparticles offered a considerable improvement in the performance characteristics of the sensors. FESEM and HRTEM were used to characterize the structure of the new nanoparticle. EIS showed that decreasing the resistance caused improvement of sensor potential reading. The fabricated sensors are good candidates for CDB micro determination in real samples with high accuracy and precision.

References

1. M. R. Siddiqui, Z. A. AlOthman, N. Rahman, *Arab. J. Chem.*, 10 (2017) S1409.
2. A. Doki, S. K. Kamarapu, *Int. J. Pharm. Biol. Sci.*, 3 (2013)152.
3. A. Pathak, P. Rai and S. J. Rajput, *J. Chromatogr. Sci.*, 48 (2010) 235.
4. M. I. Toral, P. Richter, N. Lara, P. Jaque, C. Soto, M. Saavedra, *Int. J. Pharm.*, 189 (1999) 67.

5. S. A. Ozkan, N. Erk, Z. SentÜrk, *Anal. Lett*., 32 (1999) 497.
6. A. S. Amin, H. A. Dessouki, M. M. Moustafa, M. S. Ghoname, *Chem. Pap*., 63 (2009)716.
7. M. R. Khoshayand, H. Abdollahi, A. Moeini, A. Shamsaie, A. Ghaffari, S. Abbasian, *Drug Test. Anal*., 2 (2010) 430.
8. B. Nickerson, *J. Pharm. Biomed. Anal*., 15 (1997) 965.
9. A. Sheibani, M. R. Shishehbore, Z. T. Ardakani, *Chin. Chem. Lett*., 22 (2011) 595.
10. V. V. Cosofret, R. P. Buck, Pharmaceutical Applications of Membrane Sensors, CRC Press, Boca Raton, FL, (1992).
11. K. Vytras, Encyclopedia of Pharmaceutical Technology, J. Swarbrick, J. C. Boylan, (1995) *Marcel Dekker, New York*, 347-388.
12. S. A. Ozakan, Electroanalytical Methods in Pharmaceutical Analysis and Their Validation, 14 (2011), *HNB Publishing, New York.*
13. V. K. Gupta, A. Nayak, S. Agarwal, B. Singhal, *Comb. Chem. High Throughput Screening*. 14 (2011) 284.
14. A. Karimi, F. Faridbod, L. Safaraliee, *Anal. Bioanal. Electrochem*., 3 (2011) 532.
15. S. Mesaric, E. A. M. F. Dahmen, *Anal. Chim. Acta*, 64 (1973) 431.
16. T. S. Anirudhan, S. Alexander, *Biosens. Bioelectron*., 64 (2015) 586.
17. M. M. Khalil, W. M. A. El Rouby, I. H. Abd-Elgawad, *IEEE Sensors J*. 18 (2018) 3509.
18. K. Kor, K. Zarei, *Electroanalysis*, 25 (2013) 1497.
19. Bo. Fu, T. Liu, J. Chen, K. Li, *Sens. Actuat. B: Chem.*, 272 (2018) 598.
20. S. V. Kurkov, T. Loftsson, *Int. J. Pharm*., 453 (2013) 167.
21. S. M. Saad, E. M. Eman, *Anal. Chem*., 61 (1989) 2189.
22. J. Gallardo-González, A. Baraket, A. Bonhomme, N. Zine, M. Sigaud, J. Bausells, A. Errachid, *Anal. Lett*., 51 (2018) 348.
23. El. Khaled, H. N. A. Hassan, M. Ahmed, R. O. El-Attar, *Electroanalysis*, 29 (2017) 975.
24. A. Khodadadi, E. Faghih-Mirzaei, H. Karimi-Maleh, A. Abbaspourrad, S. Agarwal, V. K. Gupta, *Sens. Actuat. B: Chem*., 284 (2019) 568.
25. J. B. Raoof, R. Ojani, H. Karimi-Maleh, *J Appl. Electrochem*., 39 (2009) 1169.
26. D. Tonelli, E. Scavetta, I. Gualandi, *Sensors*, 19 (2019)1186.
27. T. K. Aparna, R. Sivasubramanian, *J. Chem. Sci*., 130 (2018) 27.
28. M. DoulacheL, M. Trari, B. Saidat, *J. Chem. Sci.*, 130 (2018)110.
29. W. G. Hozayen, A. M. Mahmoud, E. M. Desouky, E.S. El-Nahass, H. A. Soliman, A. A. Farghali, *Biomed. Pharmacother*. 109 (2019) 2527.
30. H. Lia, X. Wu, B. Yang, J. Li, L. Xu, H. Liu, S. Li, J. Xu, M. Yang, M. Wei, *Mater. Sci. Eng. C*., 94 (2019) 453.
31. A. Watermann, J. Brieger, *Nanomaterials (Basel)*, 7 (2017) E189.
32. J. Wen, K. Yang, F. Liu, H. Li, Y. Xu, S. Sun, *Chem. Soc. Rev*., 46 (2017) 6024.
33. X. Wang, X. Li, A. Ito, Y. Sogo, T. Ohno, *Acta Biomater*., 9 (2013) 7480.
34. R.K. Singh, K.D. Patel, K.W. Leong, H.W. Kim, *ACS Appl. Mater. Interfaces*, 9 (2017) 10309.
35. D. S. Moon, J. K. Lee, *Langmuir*, 28 (2012) 12341.
36. M. M. Khalil, Y. M. Issa, A. G. Mohamed, *Electroanalysis*, 26 (2014) 2789.
37. M. M. Khalil, W. M. A. El Rouby, M. A. Korany, *Mater. Sci. Eng C*., 100 (2019)186.
38. M. M. Khalil, Y. M. Issa, G. A. El Sayed, *RSC Adv*., 5 (2015) 83657.
39. A. Sabatini, A. Vacca, P. Gans, *Talanta*, 21 (1974) 53.
40. R. P. Buck, E. Lindner, *Pure Appl. Chem.*, 66 (1994) 2527.
41. Y. Umezawa, K. Umezawa, H. Sato, *Pure Appl. Chem.*, 67 (1995) 507.
42. M. Shamsipur, A. A. Miran Beigi, M. Teymouri, S. Rasoolipour, Z. Asfari, *Anal. Chem.*, 81 (2009) 6789.
43. E. Bakker, E. Pretsch, *Anal. Chem.*, 74 (2002) 420 A.
44. E. Bakker, *J. Electrochem. Soc.*,143 (1996) L83.

45. E. Bakker, *Anal. Chem.*, 69 (1997) 1061.
46. Y. I. Korpan, M. V. Gonchar, A. A. Sibirny, C. Martelet, A. V. El'skaya, T. D. Gibson, A. P. Soldatkin, *Biosens. Bioelectron*., 15 (2000) 77.